A Spaceborne Calibration Spectrometer

Jie Wang, Yue Ma, and Shaofan Tang

Abstract The spaceborne calibration spectrometer is a specialized cross-calibration payload in orbit. It was equipped on the HY-1C satellite and had been launched in 2018 (Yang, Chin. Space Sci. Technol. 5:2, 2011). It achieves a high signal-to-noise ratio and the capability of large dynamic detection through the grating spectrometer and high full-well detector. Using the sun and diffuser as the light source, the spectrometer achieves high radiometric and wavelength calibration accuracy through the full aperture and all lightpath solar calibration. The method of spectrum reconstruction is adopted to achieve the high accuracy of cross-calibration when the spectrometer obtains the same ground-image which is detected by a calibrated remote sensor at the same time. It will help to improve the quantitative level of the calibrated remote sensor. The on-orbit test results show that the accuracy of radiation calibration is 2%, the accuracy of wavelength calibration is less than 0.5 nm, and the accuracy of cross-calibration is less than 5%.

1 Introduction

Hyperspectral imaging sensor can obtain 3-dimensional data cube which includes 2-dimensional image and 1-dimensional spectral data. It has the ability to detect geometric, radiative, and spectral characteristics of the target. Because of this, hyperspectral imaging technology became an advanced method of earth observation. In order to improve the quantification level of HY-1C [1], the hyperspectral imaging sensor can be used to achieve the function of cross-calibration. Recently, the main spectrometer which is classified by light-splitting elements includes diffraction grating imaging spectrometer and prism imaging spectrometer [2, 3].
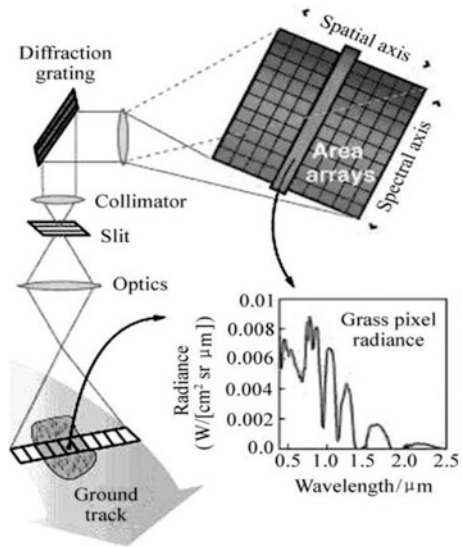
J. Wang (✉) · Y. Ma · S. Tang
Beijing Key Laboratory of Advanced Optical Remote Sensing Technology, Beijing Institute of Space Mechanics and Electricity, Beijing, People's Republic of China

Fig. 1 Principle diagram of hyperspectral imaging

Along with the development of manufacture capability of light-splitting element, high-speed array CCD or CMOS, large volume data processing, we have the ability to design and manufacture the spectrometer which has the characteristics of high precision, high stability, high spatial and spectral resolution, and high signal-to-noise ratio [4] (Fig. 1).

Nowadays, the spaceborne cameras are developed in the direction of large aperture, high resolution, and high quantification. To achieve the high quantification, the calibration equipment must be set in the camera, but the calibration equipment which is too large does not have enough space. Some payload which doesn't have calibration device need the camera, such as MODIS which is high stability, to achieve cross calibration and correct the calibration coefficient. In this way, the calibration accuracy will be affected, because of the difference of the observation time, the target and spectral response function between the camera and the spectrometer (Fig. 2).

2 System Function, Performance, and Composition

The purpose of the spectrometer is to calibrate another camera, so it must be high precision, high signal-to-noise ratio, and stability. As a result, the index of the equipment is shown in Table 1.

The spaceborne calibration spectrometer has two main functions: Firstly, it can obtain the image and spectral data of the earth to cross calibrate with another camera. Secondly, it can get the radiant energy from the diffuser which can reflect the
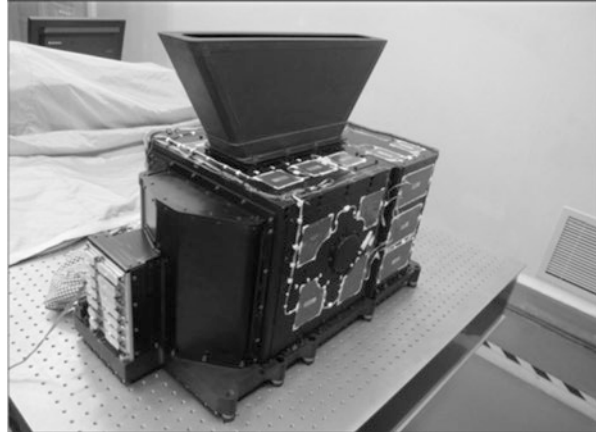
Fig. 2 The spaceborne
calibration spectrometer

Table 1 The index of the
spectrometer

Serial number	Name of the index	Target value
1	Wavelength range	0.4–0.9 μm
2	Swath	12.1 km
3	Spectral resolution	5.2 nm
4	Observation modes	Nadir
5	SNR@typical	>1000
6	Radiometric accuracy	2%
7	Accuracy of wavelength	<0.5 nm
8	Accuracy of cross-calibration	5%

energy of the solar. Especially, the lightpath of solar calibration includes sun, screen, and diffusing panel.

Because of these functions, the spectrometer has two channels. The two channels can be switched by a rotating mechanism which includes two mirrors. When one mirror turns an angle, the other mirror turns half to keep the direction of the light. The depolarizer is before the rotating mechanism, it can eliminate the polarization of incoming light. The fore optics and Offner spectrometer split the light and CCD detects the 2-dimensional signal, one-dimensional is the image and the other is the spectrum. The system composition is shown in Fig. 3.

3 Characterization

3.1 Large Dynamic Range and High SNR

The spectrometer is used as standard equipment to supply data which is used for the calibrated camera. Because of this, the subsystem must own high dynamic range and high SNR. On the other hand, the target of the spectrometer is the ocean, so the
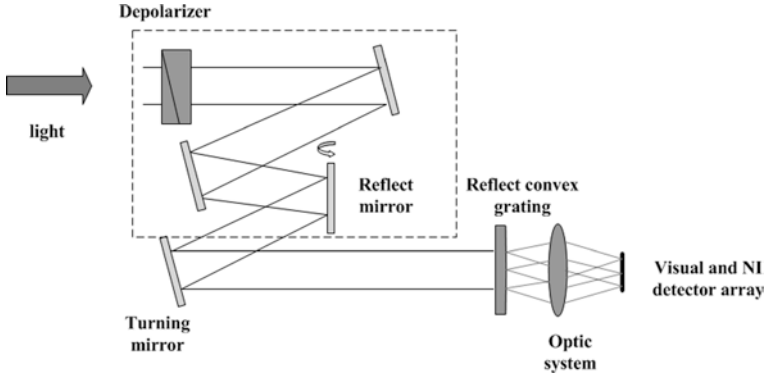
Fig. 3 The system composition

payload also needs a high dynamic range and SNR. When the equipment was designed, we used the below formulation to compute the signal-to-noise ratio of the system, the formulation is shown below:

$$\frac{S}{N} = \frac{\pi}{4} \cdot L(\lambda) \frac{\tau(\lambda) \cdot T \cdot A \cdot \sigma}{\frac{\mathrm{hc}}{\lambda} \cdot N \cdot F^2} \cdot \eta(\lambda) \cdot \mathrm{CVF} \cdot \Delta\lambda \qquad (1)$$

From the formulation, there are six main elements which can affect the result of the system.

1. F# of the optics;
2. Diffraction efficiency of grating;
3. Optical transmittance;
4. Quantum efficiency of the detector;
5. The noise of the detector;
6. The noise of the circuit;
7. Full well of the detector.

Decreasing the F# of the subsystem can get more incoming energy; however, the volume and weight of the spectrometer will get larger. The diffraction of grating, optical transmittance, quantum efficiency, noise of the system, and the full well are limited by the level of the technology. When the subsystem is designed, we need to consider all these factors. According to the design, the test result is shown in Fig. 4.
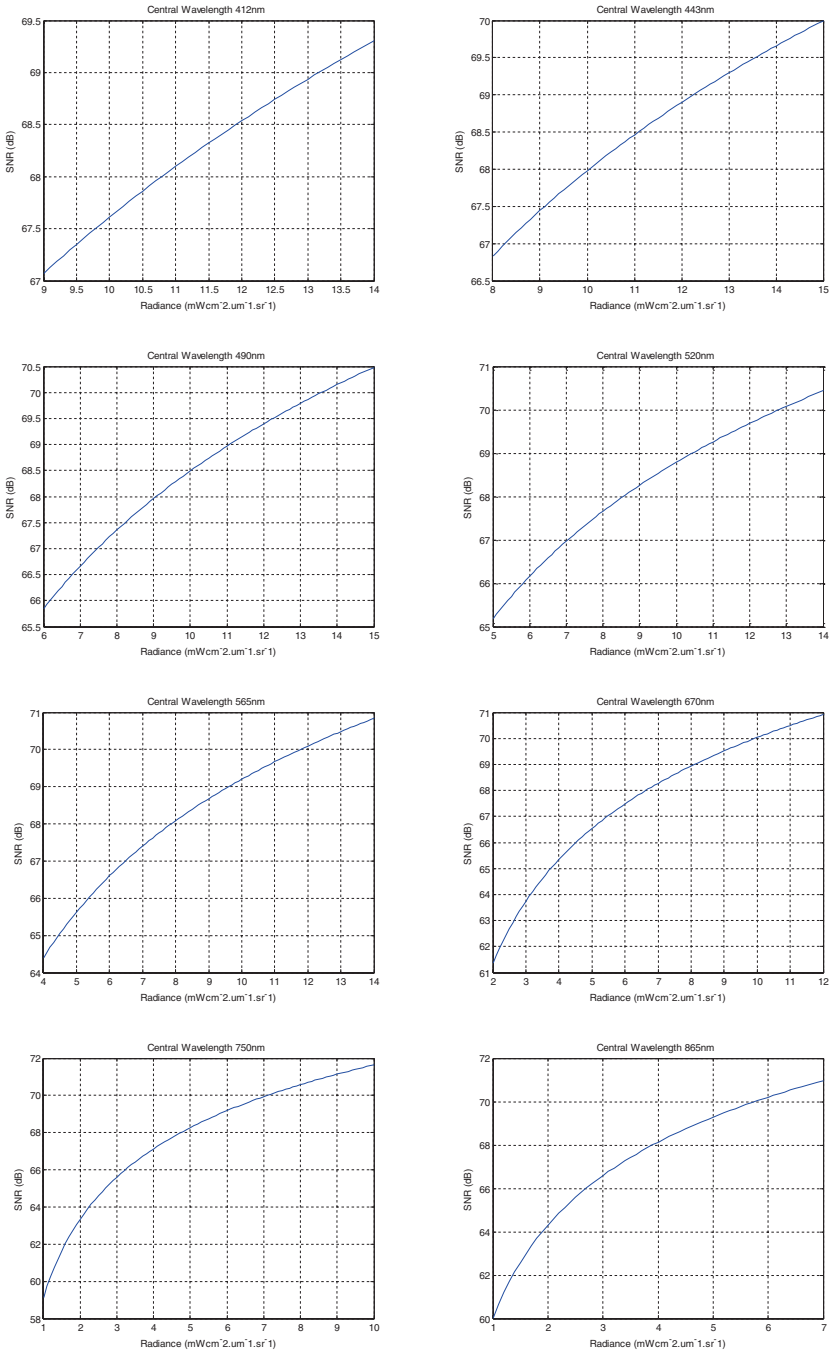
Fig. 4 The SNR results

3.2 High Precision On-board Calibration

The method of solar calibration is adopted to achieve high accuracy radiation calibration and wavelength calibration. The light source consists of solar, screen, and diffuser. The diffuser includes radiation diffuser and wavelength diffuser to achieve different functions. The screen and diffuser are shown in Fig. 5.

3.2.1 Calibration Timing

In order to avoid the stray light from the earth, the calibration timing is set at the moment when the satellite can detect the solar energy and beneath the satellite the areas are still in the darkness. The simulated result in STK is shown in Fig. 6.

The design of the sun baffle is needed to concern, because the zenith and azimuth of incoming light are various in every on-board calibration test. The variation of the altitude and azimuth is shown in Fig. 7.
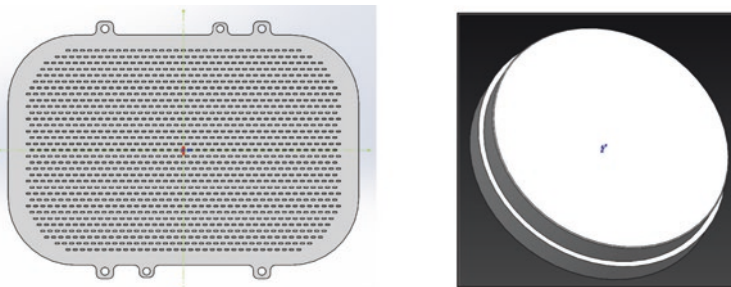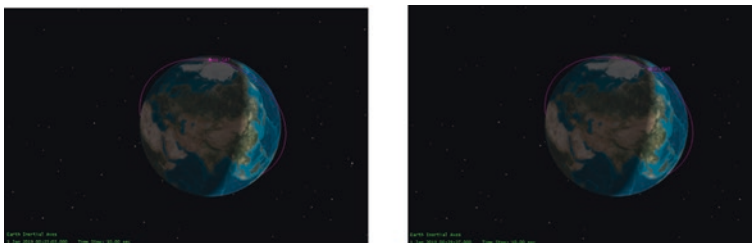

Fig. 5 The screen and diffuser

Fig. 6 The simulated result in STK
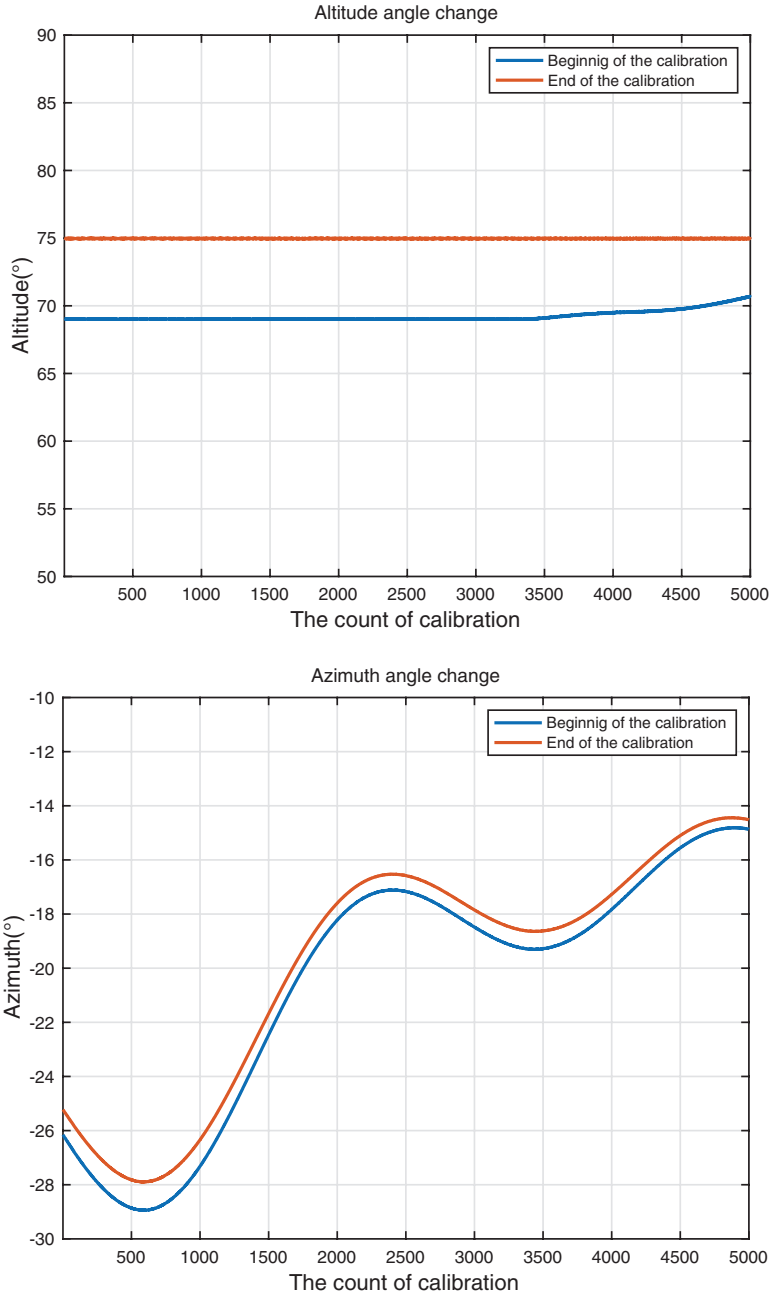
Altitude angle change

Azimuth angle change

Fig. 7 The variation of the altitude and azimuth

3.2.2   In-Orbit Radiation Calibration Process

In the lab, the model of the radiometric diffuser plane should be built, it includes the BRDF of the diffusers, the solar input angle, and the solar irradiance. Meanwhile, the spectrometer requires accurate absolute and inter-band radiometric calibration to get the calibration coefficient. The formulation is shown below:

$$L_{CAL} = \frac{E_s(\lambda) \times \cos\theta}{R(t)^2} \cdot f_{cal} \cdot \tau \tag{2}$$

In-orbit, according to solar input angle, satellite attitude, and solar irradiance data, the irradiance of the sun on the calibration plate is obtained. The formulation is shown below:

$$F_{i,j} = \frac{L_{cal}}{L_{lab}} \tag{3}$$

Compared with the irradiance which is computed by using the calibration equation and the theoretical model result, the irradiance correction factor can be obtained, it is shown below:

$$L_{TG} = F_{i,j} \times L_{lab} \tag{4}$$

Finally, the calibration equation of the spectrometer is shown below:

$$DN_i = F \times K_i \times L_i + B_i \tag{5}$$

Radiometric calibration accuracy of the spectrometer is less than 2%.

3.2.3   In-Orbit Wavelength Calibration Process

The spaceborne calibration spectrometer achieves the high precision wavelength calibration based on the wavelength diffuser which contains rare earth. There are several characteristic absorption peaks in the whole spectrum [5].

   In the lab, the spectral reflectivity of the radiometric diffuser and wavelength should be measured. At the same time, the spectrum response function should be accurately detected in a small step (<1 nm), the result is shown in Fig. 8.

   Construct the theoretical ratio of the radiometric diffuser and wavelength diffuser, the ratio is shown below:

$$V(i) = \int_{\infty}^{-\infty} \frac{\rho(\lambda)}{\gamma(\lambda)} \cdot R(\lambda - \lambda_c^i) d\lambda \tag{6}$$

According to the data of spectrometer, the actual ratio can be obtained. According to construct a pricing function, we could get the central wavelength and wavelength
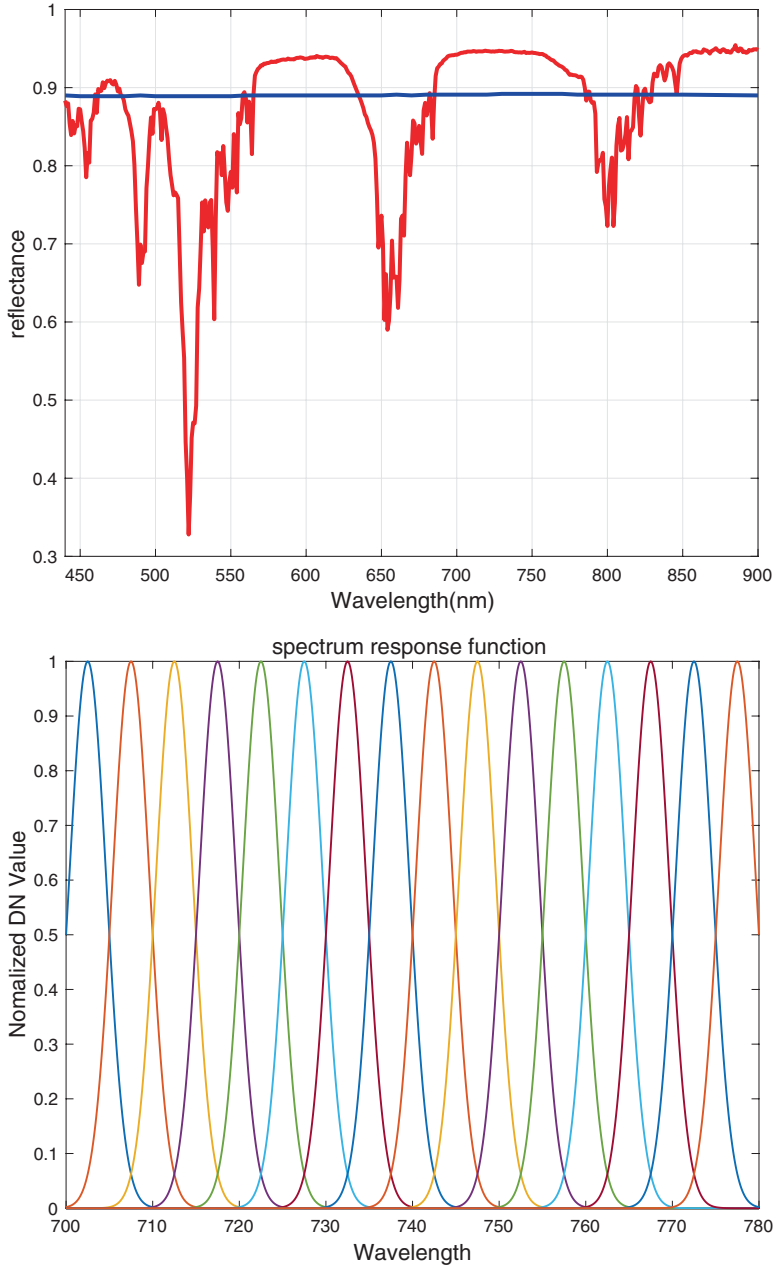
Fig. 8 Spectral reflectivity and spectrum response function

drift when the value of the pricing function is minimal, the central wavelength and wavelength drift can be confirm. The formulation of the function is shown below:

$$\Delta_i = \frac{\sum_{j=-N}^{j=N}\left(M(i+j)-\bar{M}\right)\times\left(V(i+j)-\bar{V}\right)}{\sqrt{\sum_{j=-N}^{j=N}\left(M(i+j)-\bar{M}\right)\times\left(M(i+j)-\bar{M}\right)}\sqrt{\sum_{j=-N}^{j=N}\sum_{j=-N}^{j=N}\left(V(i+j)-\bar{V}\right)\times\left(V(i+j)-\bar{V}\right)}} \tag{7}$$

According to the dispersion model, the relationship between the number of the pixel and central wavelength is shown below:

$$\lambda_c^i = a\cdot i + b \tag{8}$$

So the central wavelength drift is shown below:

$$\lambda_{c\_cor}^i = \lambda_c^i + \Delta\lambda \tag{9}$$

According to the on-board test, the wavelength calibration accuracy is 0.5 nm.

3.3 Cross-Calibration

The influence factors of cross-calibration accuracy include the calibration uncertainty of the spectrometer, spectral matching factor uncertainty, the calibration uncertainty of the target load, and another unknown uncertainty. The spectral matching factor uncertainty consists of earth object matching uncertainty, the time matching uncertainty, the geometric matching uncertainty, and spectral response matching uncertainty. In order to improve the accuracy of the cross-calibration, the method based on the spectrum recovery is adapted (Fig. 9).
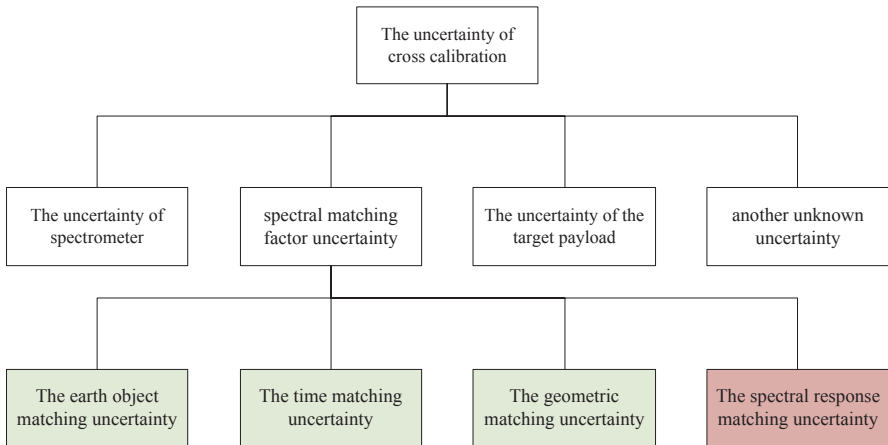

Fig. 9 The influence factors of cross-calibration

The same target is imaged simultaneously with the spectrometer and the target load, which have completed high precision radiation calibration and wavelength calibration. The discrete spectral radiance can be obtained by the calibration equation of the spectrometer after on-orbit correction. Then the continuous spectral radiance is obtained by interpolation and iteration. Through the continuous spectral radiance, the target load is cross-calibrated. The key point is how to get continuous spectral radiance. According to the absolute calibration equation, we can get the discrete spectral radiance, it is shown below:

$$DN_i = K_i \times L_i + B_i \tag{10}$$

Through data interpolation, we can get the initial continuous spectral radiance.

$$L^0 = L = \{L_i \mid (i = 1, 2, 3, \ldots, n)\} \tag{11}$$

$$L^0(\lambda) = \text{spline\_interp}(L^0) \tag{12}$$

The error is reduced by iteration, and the continuous spectrum is obtained when the error judgment condition is satisfied. The iteration formula is as follows:

$$L_i^k = \sum L^k(\lambda) S(\lambda) / \sum S(\lambda) \tag{13}$$

$$L^k = \{L_i^k \mid (i = 1, 2, 3, \ldots, n)\} \tag{14}$$

$$L^{k+1} = L_I^k + a(L - L^k) \tag{15}$$

$$L^{k+1} = \text{spline\_interp}(L^k) \tag{16}$$

Error judgment condition is shown below:

$$L^k - L_2 \ll 10^{-6} \tag{17}$$

After a comprehensive analysis of the indicators, the accuracy of cross-calibration is less than 5%.

4 Application

The spectrometer has large dynamic detection capability, high signal-to-noise ratio, and high stability. It can be used as a special calibration instrument for large diameter and high-resolution payload. These instruments are usually limited by volume and weight, so it is difficult to design calibration lightpath and calibration device [6].

On the other hand, the load is capable of graph and spectrum detection with high signal-to-noise ratio, and its spectrum can be extended to 2.5 um. The data can be used for atmospheric correction of the calibrated payloads.

5 Conclusion

The on-board calibration spectrometer is the first imaging spectrometer dedicated to calibration on the same platform. The spectrometer owns the large dynamic range, high SNR, and high accurate radiometric calibration and wavelength calibration. It provides a solution for quantitative increase of large camera on the same platform.

References

1. Yang, B.: Constructing China's ocean satellite system to enhance the capability of ocean environment and disaster monitoring. Chin. Space Sci. Technol. **5**, 2 (2011)
2. Yang, Z.-p., Tang, Y.-g., Bayanheshig, Ji-cheng, C., Yang, J.: Research on small-type and high-spectral-resolution grating monochromator. Spectrosc. Spectr. Anal. **36**, 273 (2016)
3. Yan, L.-w.: Study and design on Dyson imaging spectrometer in spectral broadband with high resolution. Spectrosc. Spectr. Anal. **34**, 1135 (2014)
4. Sun, J.-m., Guo, J., Shao, M.-d., Jin-song, Y., Zhu, L., Gong, D.-p., Qi, H.-y.: Precise focusing for TDICCD camera with wide field of view. Optics Precis. Eng. **22**, 3 (2014)
5. Chen, H.-y., Zhang, L.-m.: Spectral calibration for dispersive hyperspectral sensor based on doped reflectance standard panel. Optics Precis. Eng. **12**, 2643 (2010)
6. Du, X.-w., Shen, Y.-c., Li, C.-y., An, N., Shi, Y.-j., Wang, Q.-p.: EUV flat field grating spectrometer and performance measurement. Spectrosc. Spectr. Anal. **8**, 2272–2273 (2012)